

BOTD: Bold Outline Text Detector

Chuang Yang, Zhitong Xiong, Mulin Chen, Qi Wang*, Xuelong Li

School of Computer Science and Center for OPTical IMagery Analysis and Learning (OPTIMAL),
Northwestern Polytechnical University

cyang113@mail.nwpu.edu.cn, xiongzhitong@gmail.com, chenmulin@nwpu.edu.cn,

crabwq@gmail.com, xuelong_li@nwpu.edu.cn

Abstract

Recently, text detection for arbitrary shape has attracted more and more search attention. Although segmentation-based methods, which are not limited by the text shape, have been studied to improve the performance, the slow detection speed, complicated post-processing, and text adhesion problem are still limitations for the practical application. In this paper, we propose a simple yet effective arbitrary-shape text detector, named *Bold Outline Text Detector (BOTD)*. It is a novel one-stage detection framework with few post-processing processes. At the same time, the text adhesion problem can also be well alleviated. Specifically, *BOTD* first generates a center mask (CM) for each text instance, which makes the adhesive text easy to distinguish. Base on the CM, we further compute the polar minimum distance (PMD) for each text instance. PMD denotes the shortest distance between the center point of CM and the outline of the text instance. By dividing the text mask into CM and PMD, the outline of arbitrary-shape text instance can be obtained by simply predicting its CM and PMD. Without any bells and whistles, *BOTD* achieves an F-measure of 80.1% on CTW1500 with 52 FPS. Note that the post-processing time only accounts for 9% of the whole inference time. Code and trained models will be publicly available soon.

1. Introduction

Image text contains rich and accurate high-level semantic information, which is the key element to understand the scene through an image. If the text area in the image can be detected accurately, it will be of great help in understanding the image information. Numerous methods [1, 2, 3, 4, 5, 6, 7, 8] have been achieved remarkable performance on the problem of horizontal and multi-oriented text detection. Therefore, more and more researchers shift their focuses on the problem of arbitrary-shape text detection [9, 10, 11, 12]. Since regression-based text detec-

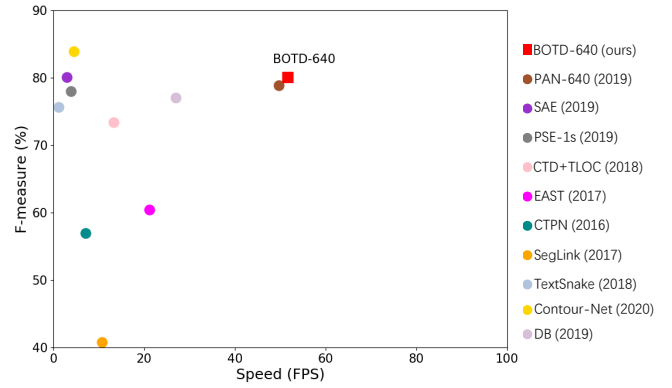


Figure 1. The performance and speed on curved text dataset CTW1500. Our method achieves the ideal tradeoff between effectiveness and efficiency.

tion methods have certain limitations for arbitrary-shape text detection. Therefore, most of the works tend to complete the detection of arbitrary-shape text by segmentation methods. However, there are three main challenges in segmentation-based arbitrary-shape text detection methods: 1) segmentation-based text detection methods are pixel-to-pixel to predict the categories of all pixels in an image. This is luxurious for practical application scenarios that pursue both speed and accuracy; 2) most segmentation-based methods need to get the text region according to the classified pixels through complex post-processing; 3) in the real world, it is common for different text instances to be closely connected, i.e., the text adhesion problem. Therefore, the model and post-processing steps of segmentation-based methods are both more complicated than regression-based methods.

The detection of arbitrary-shape text through a simple model with few post-processing steps will have a great practical significance owing to the real-time speed. Therefore, we propose a simple yet effective arbitrary-shape text detector named *Bold Outline Text Detector (BOTD)*.

BOTD is a single-shot text detection model, which detects text instances by bolding the width of the Center Mask (CM) outline from one pixel to Polar Minimum Distance (PMD). Compared with the polygon regression methods, BOTD has a very elegant, brief model structure to detect arbitrary-shape text in an end-to-end manner. By this means, the accumulation error caused by multiple detection process can be avoided. Compared with segmentation-based methods, the proposed method combines the advantages of regression-based and segmentation-based methods. Specifically, we reduce the model complexity by framing the segmentation problem into a regression problem based on a single-stage detection framework, which greatly simplifies the post-processing steps and improves the testing speed. As we can see from Fig. 1, the testing speed is significantly accelerated while high-quality detection results are maintained.

The contributions of this work are summarized as follows:

1. An anchor free one-stage detection framework for arbitrary-shape text detection is proposed, which combines the idea of regression with segmentation and can significantly speed up the detection process.
2. The proposed method takes advantage of the polar symmetry characteristic (PSC) of CM, which can simplify the model complexity and reduce post-processing steps while maintaining good detection performance.
3. By modeling the text mask into CM and PMD, the proposed method can easily improve the detection performance of texts that are very close to each other.
4. The PMD IoU Loss is designed in this work. Experiments prove that PMD IoU Loss is not only easier to converge, but also greatly improves the accuracy compared with existing Dice Loss [13] and Smooth- l_1 Loss.

2. Related Work

In recent years, deep learning is rapidly promoting the development of the text detection field. These deep learning-based text detection methods can be classified into the two following categories: regression-based methods and segmentation-based methods.

2.1. Regression-based methods.

Great achievements have been made in the field of general object detection, such as the classic object detection method Faster-RCNN [14]. It brings great inspiration to researchers in the field of text detection, and some text detection methods [5, 6, 7, 8, 15, 16, 17] based on it are proposed. However, due to the slow speed of two-stage detec-

tion methods, more and more one-stage general object detection methods [1, 2, 3, 4] based on SSD [18] and YOLO [19] are proposed. But the width to height ratio of text instance varies greatly, which leads to general object detection methods cannot directly achieve good performance when detecting text. To adapt to the variable aspect ratio of text, Textboxes [20] uses 1×5 convolution kernel instead of 3×3 convolution kernel to extract text region features more effectively. Moreover, it increases the proportion of default boxes to cover more different scales texts. Textboxes++ [21] predicts the offset of multi-oriented text relative to horizontal text boxes based on Textboxes, to achieve better detection performance of multi-oriented text. Although one-stage methods have been improved in speed compared with two-stage methods, they still need to set a lot of anchors in advance to cover as many texts as possible, which increases model complexity and slows down its speed. Therefore, anchor free text detection methods [22, 5, 23, 24, 25, 26] have attracted people's attention. EAST [27] realizes anchor free text detection by predicting the distance between each pixel position and the text border, which brings great inspiration for researchers. However, these methods are limited in the detection of arbitrary shape text, such as curved shapes.

2.2. Segmentation-based methods.

Because the regression-based methods are limited by text shapes, researchers have gradually begun to use segmentation-based methods [28, 9, 10, 11, 12] to detect arbitrary-shape text. Zhang et al. [29] use text block FCN to detect text blocks and the multi-directional text line, and then character centroid FCN are combined to get the final text box. Yao et al. [30] generate saliency map, character area, and connection direction of text block, and then accurate prediction results are obtained through a series of complicated post-processing procedures. Although these segmentation-based methods have achieved good performance when detecting arbitrary-shape text. While the overall performance of these methods is limited by the complicated model and a lot of post-processing processes. Although LSAE [31] reduces the model complexity and finds a solution to the text adhesion problems, it still needs a series of complex post-processing steps to get the final text outline.

3. Methodology

In this section, we introduce the overall structure of the proposed BOTD firstly. Then, PMD and CM are explained through illustrations. Next, the reconstruction process of the text instance mask through CM and PMD are described in detail. At last, the proposed PMD IoU Loss and its advantages compared with other Loss are elaborated.

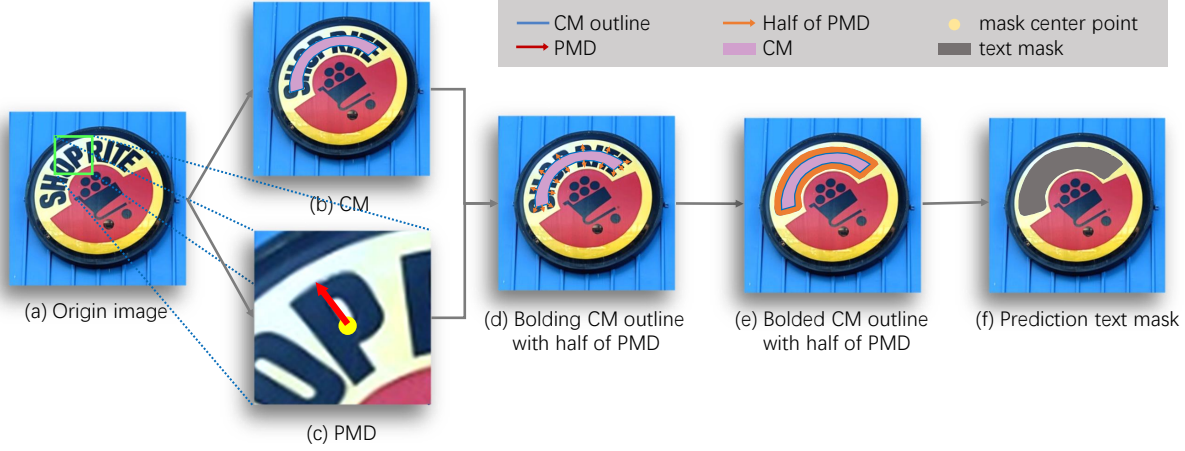


Figure 2. The procedure of bold CM outline to get text instance. (b), (c) are CM and PMD obtained by (a), respectively. The blue outline in (b) is the original outline of CM. By bold the width of the outline from one to half of PMD, the result (d) that after bold the outline based on CM can be obtained. The white mask in (e) is the text instance mask.

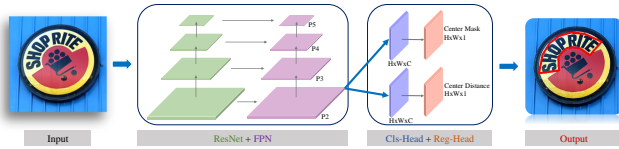


Figure 3. The overall pipeline of BOTD. ResNet and FPN are used to extract multi-scales features of Input. Cls-Head and Reg-Head are for classification and regression respectively with $H \times W \times 1$ size.

3.1. Overall Pipeline

The architecture of BOTD is shown in Fig. 3, which is a simple yet effective end-to-end framework. It is composed of ResNet [32], feature pyramid network (FPN) [33], and two tasks-specific heads. We firstly use ResNet as backbone to extract the basic image feature. Then, the multi-scales image feature output from FPN. Next, two tasks specific heads generate CM and PMD through the multi-scales image feature. Finally, text mask can be generated by bolding the CM outline from one pixel to PMD. Although there are lots of effective auxiliary structures to improve model performance. We only use ResNet and FPN to show the simplicity and effectiveness of our method.

3.2. PMD and CM

Firstly, we describe PMD in detail. As we can see from Fig. 4, the polar coordinate axis is established by taking the center point of the text mask as the origin. PMD is the shortest distance between the center point of text mask and text outline in 360-degree directions such as the red arrow. To facilitate visualization, only distances between the center point and text outline along directions of 0° , 45° , 90° , 135° ,

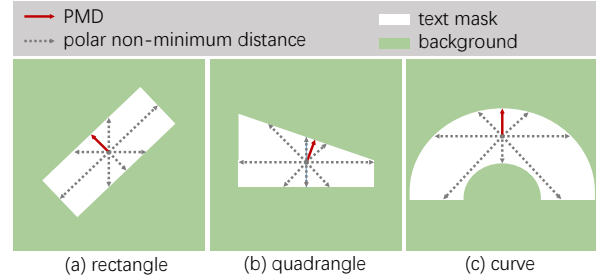


Figure 4. The red solid line is the PMD. Those gray dot lines are polar non-minimum distance. The white mask is text instance mask.

180° , 225° , 270° , 315° , and PMD are drawn.

Next, we explain CM through Fig. 5. CM (top) is different from normal shrink mask (middle) and centerline (down). For CM, the shortest distance between each point on the CM outline and the text mask outline within 360-degree is half of PMD. And the center of CM is also the text mask center. We regard this special relationship between CM and text mask as PSC of CM. PSC is very important for us to model the arbitrary-shape text detection problem, it will be described in sec 3.3. For normal shrink mask, the shortest distances between each point on normal shrink mask outline and text mask outline within 360-degree are not equal to each other usually. This phenomenon also exists in centerline.

3.3. Reconstruct Text Instance Mask

When anchor-free text detection methods are used to detect quadrilateral text, they only need to predict the location of the center point and distances between four sides of the

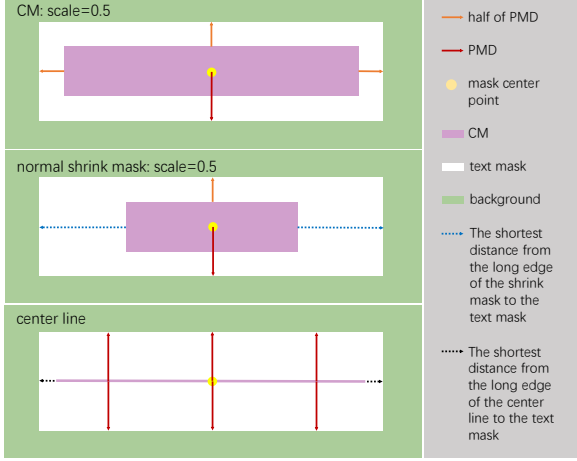


Figure 5. The shortest distances from each point on the CM (top) outline to the text mask outline are equal, however normal shrink mask and centerline are not.

text box and center point. Inspired by this idea, our method regards CM and PMD as the center point and distances respectively, and detects arbitrary-shape text by anchor free one-stage text detection framework. Specifically, as we can see from Fig. 2, BOTD generates the CM (b) and PMD (c) of someone text instance through the original image (a) firstly. Then, we get the CM outline and bolding it from one pixel to half of PMD (d). After generating the bolded CM outline with half of PMD (e), we can easily get the prediction mask (f) by picking those pixels that do not belong to the background. The method greatly reduces the model complexity and post-processing steps. More importantly, it provides a new way for the problem of arbitrary-shape text detection.

3.4. Loss Function

For learning BOTD, the loss function is formulated as:

$$L = L_{cls} + \lambda L_{reg}, \quad (1)$$

where L_{cls} and L_{reg} denote classification loss and regression loss respectively. Moreover, we use the balance weight parameter λ to represent the importance of two losses. It always set 1 in our method.

For classification task, the goal is to maximize the IoU between prediction CM and ground-truth CM. Cross entropy is generally used as classification loss function in segmentation. However, it leads to the unity deviation between the optimization objective and the loss function. Dice coefficient [13] is a set similarity measure function, which is usually used to calculate the similarity of two samples. In our classification task, the prediction CM and ground-truth CM can be regarded as two samples to calculate the similarity. Therefore, using the dice coefficient as the classification

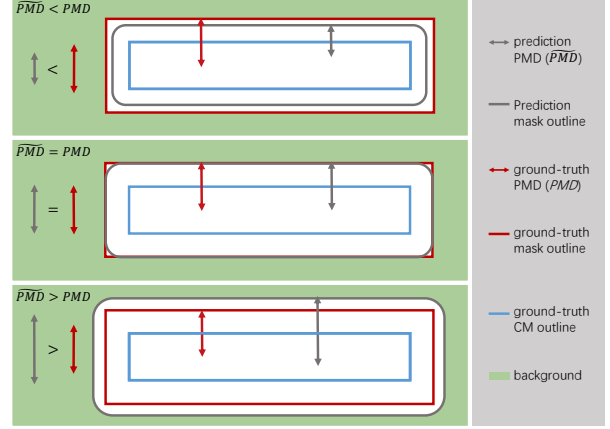


Figure 6. Illustration of PMD IoU. The red arrow and gray arrow are ground-truth PMD and predicted PMD respectively. From top to bottom are PMD IoU of predicted PMD and ground truth PMD under bigger, equal and smaller conditions

loss function enhances the integrity between the optimization objective and the loss function compared with the cross entropy. The Dice Loss is defined as followed:

$$L_{cls} = 1 - \frac{2 \times |X \cap Y| + 1}{|X| + |Y| + 1}, \quad (2)$$

where X, Y denote the predicted and ground-truth CM respectively. Because the denominator repeats the calculation of common elements between X and Y , the coefficient of the molecule here set 2. At the same time, to avoid the problem that the molecule is divided by 0 when X and Y are both zero, a constant is added to both the numerator and denominator respectively. Here, we set the constant as 1.

For regression task, optimization objective is to make predicted PMD (\widehat{PMD}) equal to ground-truth PMD (PMD). Here, we introduce PMD IoU Loss starting from the definition of IoU, which is the ratio of interaction area over union area between the predicted text mask and ground-truth. From Fig. 6 we can see that there are three situations: 1) $\widehat{PMD} < PMD$ (top); 2) $\widehat{PMD} = PMD$ (middle); 3) $\widehat{PMD} > PMD$ (down). As we mentioned in sec 3.3, the predicted text mask reconstruction process by CM and PMD can be regarded as the process of bolding CM outline from one pixel to PMD. The text mask IoU can be expressed approximately by mathematical formulas as follows:

$$\text{prediction} = \int_0^{P_{CM}} \left(\frac{\widehat{PMD}}{2} \right) dl + S_{CM}, \quad (3)$$

$$\text{ground} - \text{truth} = \int_0^{P_{CM}} \left(\frac{PMD}{2} \right) dl + S_{CM}, \quad (4)$$

where *prediction* and \widetilde{PMD} are predicted text mask area and PMD. *ground-truth* and PMD are ground-truth text mask area and PMD. P_{CM} and S_{CM} denote the perimeter and area of CM respectively. The discretization of (3) and (4) can be expressed as:

$$\text{prediction} = \frac{1}{2} \sum_1^n \widetilde{PMD} + S_{CM}, \quad (5)$$

$$\text{ground-truth} = \frac{1}{2} \sum_1^n PMD + S_{CM}, \quad (6)$$

where n represents the number of points on the CM outline. Since the *prediction* and *ground-truth* are computed based on the outline of ground-truth CM, the IoU of *prediction* and *ground-truth* is as follows:

$$\text{PMDIoU} = \frac{\min(\frac{n}{2}\widetilde{PMD} + S_{CM}, \frac{n}{2}PMD + S_{CM})}{\max(\frac{n}{2}\widetilde{PMD} + S_{CM}, \frac{n}{2}PMD + S_{CM})}, \quad (7)$$

combining Eqn. 5, 6, 7, Eqn. 8 can be obtained as follows:

$$\text{PMDIoU} = \begin{cases} \frac{\frac{n}{2}\widetilde{PMD} + S_{CM}}{\frac{n}{2}PMD + S_{CM}}, & \widetilde{PMD} < PMD \\ 1, & \widetilde{PMD} = PMD \\ \frac{\frac{n}{2}PMD + S_{CM}}{\frac{n}{2}\widetilde{PMD} + S_{CM}}, & \widetilde{PMD} > PMD \end{cases}, \quad (8)$$

Since n and S_{CM} are equal for *prediction* and *ground-truth*. Therefore, the PMD IoU mainly depends on \widetilde{PMD} and PMD , Inspired by [34], the PMD IoU Loss can be expressed as:

$$\text{PMDIoULoss} = \log \frac{\max(\widetilde{PMD}, PMD)}{\min(\widetilde{PMD}, PMD)}, \quad (9)$$

Compared with Smooth- l_1 Loss, PMD IoU Loss exhibits two advantageous properties: 1) The evaluation criteria of PMD IoU Loss are the same for different scales text. However, Smooth- l_1 Loss is not sensitive to small-scale text in the training process. 2) PMD IoU Loss converges faster than Smooth- l_1 Loss in the training process, and improves the overall performance by a large margin compared with it.

4. Experiments

4.1. Implementation details

We use the ResNet [32] pre-trained on ImageNet [35] as our backbone, and the image features from backbone are fused by FPN. In the training step, BOTD is trained on each official dataset for 500 epochs without any external datasets. we use SGD [36] to train the model with learning rate 1e-3,

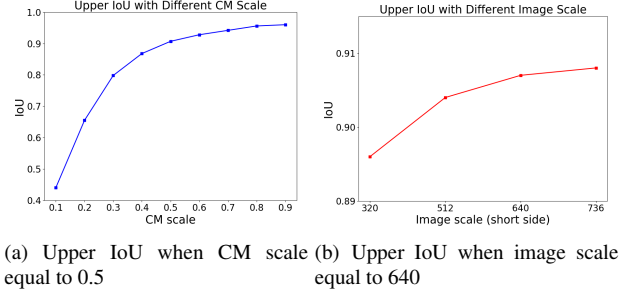


Figure 7. Upper IoU with different image and CM scale.

the momentum [37] and weight decay are 0.99 and respectively. The training batch size is set to 12 and the images are cropped to 640×640. We initialize the initial weights of FPN and head layers through [38]. For ICDAR2015, the blurred text regions labeled as DO NOT CARE are ignored in all datasets and no techniques are used to optimize loss functions, such as OHEM [39]. The data augmentation for the training dataset includes (1) random horizontal flipping; (2) random cropping; (3) random rotation with an angle range of (-10°, 10°). In the inference step, the time cost consists of the model forward time cost and the post-processing time cost.

4.2. Ablation Study

To make the conclusion of ablation studies more generalized, all experiments of ablation studies are conducted on CTW1500 (a long curve text dataset). Note that, in these experiments, all models are trained without any external dataset. we set the short sides of test images in CTW1500 and ICDAR2015 to 640 and 736 by default in the following experiments.

Upper IoU. The major concern about BOTD is that it might not depict the mask precisely. Therefore, we verify the upper IoU of BOTD as the IoU of predicted mask and ground-truth when all the prediction PMD and CM equal to ground-truth PMD and CM. Here, we use two sets of data to illustrate the situation of upper IoU in different image scales and different CM scales. From Fig. 7(a) we can see that a higher image scale brings bigger IoU. This conclusion is also applicable to the CM scale (see Fig. 7(b)), which shows that BOTD can model the mask very well.

PMD IoU Loss, Dice Loss, and Smooth- l_1 Loss In the experiment, PMD was trained with PMD IOU Loss, Dice Loss, and Smooth- l_1 Loss respectively on CTW1500. Firstly, by comparing the descent curves of Dice Loss and PMD IoU Loss (see Fig. 8(a)), it can be found that Dice Loss has been fluctuating around 0.5, and there is no convergence trend, which means that the loss function can not be used for learning PMD. While the PMD IoU Loss achieves convergence at a very fast speed. Then, by observing the descent curve of Smooth- l_1 Loss, (see Fig. 8(b)) it

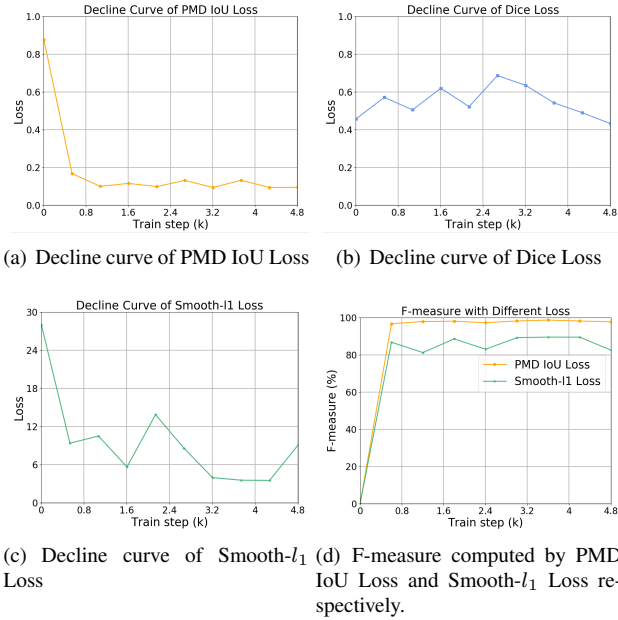


Figure 8. (a), (b), (c) are decline curve of PMD IoU Loss, Dice Loss, and Smooth- l_1 Loss respectively. (d) is detection results curve of PMD IoU Loss and Smooth- l_1 Loss with different train steps.

can be found that its range of variation is huge. And the more important thing is that Smooth- l_1 Loss measures the PMD with different scales text by calculating the absolute value of the difference between the predicted PMD and the ground-truth, which means that Smooth- l_1 Loss has different PMD standards for different scale texts. However, PMD IoU Loss considers the ratio between the predicted PMD and the ground-truth, which ensures the fairness of the network in the learning process of PMD of different scales text. From Fig. 8(c), we can see that PMD IOU Loss greatly improves the accuracy of the model compared with Smooth- l_1 Loss.

Accuracy with Different CM scale. Different CM scales usually get different accuracies. Table 1 shows the accuracies with different CM scales on CTW1500 dataset. We can see from Table 1 that the model achieves the best performance when CM scale equals 0.5. However, with the increasing or decreasing of CM scale, the model performance gradually decline. In particular, the model performance degrades dramatically when CM scale less than 0.2.

4.3. Comparison against state-of-the-art

We compare our model with other state-of-the-art methods on ICDAR2015 and CTW1500 to prove the effectiveness of BOTD. Some qualitative results on ICDAT2015 and CTW1500 are visualized in Fig. 9 and Fig. 10 respectively.

Table 1. Detection results with different settings on CTW1500 Dataset. "Scale" indicates CM scale. "P", "R", and "F" indicate precision, recall, and F-measure respectively. "Ext." means no external dataset when training model.

Backbone	Input Size	Scale	Ext.	P	R	F
ResNet18	640	0.1	×	58.0	35.5	44.0
		0.2	×	70.1	58.9	64.0
		0.3	×	77.3	69.6	73.2
		0.4	×	82.7	70.1	75.9
		0.5	×	84.8	75.9	80.1
		0.6	×	83.7	74.6	78.9
		0.7	×	82.7	71.8	76.9
		0.8	×	83.8	70.7	76.7
		0.9	×	80.5	69.0	74.3

4.3.1 Evaluation on Multi-Oriented Text Benchmark

ICDAR2015 [40] is a dataset proposed in ICDAR 2015 Robust Reading Competition, it contains 1500 images, of which 1000 are used to train the model and the remaining 500 are used to test the performance of the model. Images in this benchmark contain horizontal and oriented-texts at the same time and the image size of the training set and test set is 720×1280 .

We evaluate BOTD on the ICDAR2015 dataset and compare the detection results to state-of-the-art methods including both one-stage and two-stage models, as shown in Table 2. To ensure the fairness of the process comparison, we use ResNet-18 and ResNet-50 as backbone to compare with other methods. Specifically, we keep the feature extract part network being the same, which means the PAN-Res18 [41] detection result that we have shown in Table 2 is the result without "FPEM" and "FFM". On the one hand, without any bells and whistles, BOTD achieves the F-measure of 79.5% at an astonishing speed (36.2 FPS) when we use ResNet-18 as backbone. It surpassing all other state-of-the-art real-time detection methods. On the other hand, BOTD achieves F-measure of 80.6% at a fast speed (23.6 FPS) when we use ResNet-50 as backbone. Although the F-measure of the proposed method is slightly lower than (but still comparable to) some methods (e.g. PSENet, CRAFT), our method has a least 14 times faster speed than these methods.

4.3.2 Evaluation on Curved Text Benchmark

CTW-1500 [53] is a dataset for curve text detection. It contains 1000 images for training and 500 images for testing. The size of these images and the scale of text in the images vary greatly. Though BOTD has achieved excellent performance on the multi-oriented text benchmark, the performance of our method on the curved text benchmark is more exciting. In the same way, to ensure the fairness of the process comparison, we keep the feature extract part network being the same. This means the PAN-Res18 [41] detection result that we shown in Table 3 is the result without



Figure 9. Visualization of segmentation results on CTW1500 dataset. Green polygon and yellow polygon denote the predicted text and CM outline respectively. The red arrow denotes the PMD. (Best viewed in color.)



Figure 10. Visualization of segmentation results on ICDAR2015 dataset. Green polygon and yellow polygon denote the predicted text and CM outline respectively. The red arrow denotes the PMD. (Best viewed in color.)

Table 2. Performance Comparisons on ICDAR2015 Dataset

	Methods	Ext.	P	R	F	FPS
Methods	CTPN[42]	×	74.2	51.6	60.9	7.1
	EAST[27]	✓	83.6	73.5	78.2	13.2
	SSTD[3]	✓	80.2	73.9	76.9	7.7
	WordSup [43]	✓	79.3	77	78.2	-
	Corner [11]	✓	94.1	70.7	80.7	3.6
	RRD [44]	×	85.6	79	82.2	6.5
	MCN [45]	✓	72	80	76	-
	TextSnake [46]	✓	84.9	80.4	82.6	1.1
	PSE-1s [47]	✓	86.9	84.5	85.7	1.6
	PAN-Res18 [41]	-	-	-	78.4	33.7
	SPCNet [48]	✓	88.7	85.8	87.2	-
	CRAFT [49]	✓	89.8	84.3	86.9	-
Ours	BOTD-Res18 (736)	×	84.3	75.2	79.5	36.2
	BOTD-Res50 (736)	×	83.6	77.8	80.6	23.6

Table 3. Performance Comparisons on CTW1500 Dataset

	Methods	Ext.	P	R	F	FPS
Methods	CTPN[42]	×	60.4	53.8	56.9	7.1
	EAST[27]	×	78.7	49.1	60.4	21.2
	SegLink [2]	×	42.3	40.0	40.8	10.7
	TextSnake [46]	✓	67.9	85.3	75.6	1.1
	CTD+TLOC [50]	×	77.4	69.8	73.4	13.3
	PSE-1s [47]	×	84.8	79.7	82.2	3.9
	LSAE [31]	×	82.7	77.8	80.1	3
	PAN-Res18 [41]	×	-	-	78.8	49.7
	DB-Res18 [51]	✓	76.3	72.8	74.5	59
	DB-Res50 [51]	✓	81.6	72.9	77.0	27
	ContourNet [52]	×	84.1	83.7	83.9	4.5
	CRAFT [49]	✓	86.0	81.1	83.5	-
Ours	BOTD-Res18 (640)	×	84.8	75.9	80.1	52.5
	BOTD-Res50 (640)	×	86.3	76.8	81.3	36.7

”FPEM” and ”FFM”. DB-Res18 [41], DB-Res50 detection result that we shown in Table 3 is the result without ”DB” and ”DConv”.

As we can see from Table 3, our method achieves state-

of-the-art between real-time text detection methods with ResNet-18 backbone. Compared with PAN-Res18, BOTD outperforms it by 1.3% F-measure and is 2.8 FPS faster in speed. Although DB-Res18 is 6.5 frames faster than BOTD,

our method outperforms it by a large margin, i.e., 5.6% F-measure in performance. At the same time, BOTD with ResNet-50 backbone can run 8 times faster than ContourNet [52], and still achieve a competitive accuracy.

5. Conclusion

In this paper, we propose a simple yet effective one-stage anchor free detector for arbitrary-shape text detection. We firstly divide text mask into CM and PMD by using the PSC of CM, which not only reduces the model complexity but also avoids a lot of post-processing steps. Moreover, a novel PMD IoU loss is designed to regress PMD, which obviously improves the model performance compare with other general regression task losses. These advantages make the BOTD achieve excellent performance in both speed and accuracy. Experiments on the CTW1500 dataset demonstrate the superior advantages in speed and accuracy when compared to previous state-of-the-art text detectors.

References

- [1] Daitao Xing, Zichen Li, Xin Chen, and Yi Fang. Arbitext: Arbitrary-oriented text detection in unconstrained scene. *arXiv preprint arXiv:1711.11249*, 2017. 1, 2
- [2] Baoguang Shi, Xiang Bai, and Serge Belongie. Detecting oriented text in natural images by linking segments. In *Proceedings of the IEEE Conference on Computer Vision and Pattern Recognition*, pages 2550–2558, 2017. 1, 2, 7
- [3] Pan He, Weilin Huang, Tong He, Qile Zhu, Yu Qiao, and Xiaolin Li. Single shot text detector with regional attention. In *Proceedings of the IEEE International Conference on Computer Vision*, pages 3047–3055, 2017. 1, 2, 7
- [4] Shangxuan Tian, Shijian Lu, and Chongshou Li. Wetxt: Scene text detection under weak supervision. In *Proceedings of the IEEE International Conference on Computer Vision*, pages 1492–1500, 2017. 1, 2
- [5] Zhuoyao Zhong, Lei Sun, and Qiang Huo. An anchor-free region proposal network for faster r-cnn-based text detection approaches. *International Journal on Document Analysis and Recognition (IJDAR)*, 22(3):315–327, 2019. 1, 2
- [6] Jianqi Ma, Weiyuan Shao, Hao Ye, Li Wang, Hong Wang, Yingbin Zheng, and Xiangyang Xue. Arbitrary-oriented scene text detection via rotation proposals. *IEEE Transactions on Multimedia*, 20(11):3111–3122, 2018. 1, 2
- [7] Xiangyu Zhu, Yingying Jiang, Shuli Yang, Xiaobing Wang, Wei Li, Pei Fu, Hua Wang, and Zhenbo Luo. Deep residual text detection network for scene text. In *2017 14th IAPR International Conference on Document Analysis and Recognition (ICDAR)*, volume 1, pages 807–812. IEEE, 2017. 1, 2
- [8] Yuliang Liu and Lianwen Jin. Deep matching prior network: Toward tighter multi-oriented text detection. In *Proceedings of the IEEE Conference on Computer Vision and Pattern Recognition*, pages 1962–1969, 2017. 1, 2
- [9] Yuchen Dai, Zheng Huang, Yuting Gao, Youxuan Xu, Kai Chen, Jie Guo, and Weidong Qiu. Fused text segmentation networks for multi-oriented scene text detection. In *2018 24th International Conference on Pattern Recognition (ICPR)*, pages 3604–3609. IEEE, 2018. 1, 2
- [10] Fan Jiang, Zhihui Hao, and Xinran Liu. Deep scene text detection with connected component proposals. *arXiv preprint arXiv:1708.05133*, 2017. 1, 2
- [11] Pengyuan Lyu, Cong Yao, Wenhao Wu, Shuicheng Yan, and Xiang Bai. Multi-oriented scene text detection via corner localization and region segmentation. In *Proceedings of the IEEE conference on computer vision and pattern recognition*, pages 7553–7563, 2018. 1, 2, 7
- [12] Pengyuan Lyu, Minghui Liao, Cong Yao, Wenhao Wu, and Xiang Bai. Mask textspotter: An end-to-end trainable neural network for spotting text with arbitrary shapes. In *Proceedings of the European Conference on Computer Vision (ECCV)*, pages 67–83, 2018. 1, 2
- [13] F Milletari, N Navab, SAV Ahmadi, and V-Net. Fully convolutional neural networks for volumetric medical image segmentation. In *Proceedings of the 2016 Fourth International Conference on 3D Vision (3DV)*, pages 565–571. 2, 4
- [14] Shaoqing Ren, Kaiming He, Ross Girshick, and Jian Sun. Faster r-cnn: Towards real-time object detection with region proposal networks. In *Advances in neural information processing systems*, pages 91–99, 2015. 2
- [15] Sheng Zhang, Yuliang Liu, Lianwen Jin, and Canjie Luo. Feature enhancement network: A refined scene text detector. *arXiv preprint arXiv:1711.04249*, 2017. 2
- [16] Yingying Jiang, Xiangyu Zhu, Xiaobing Wang, Shuli Yang, Wei Li, Hua Wang, Pei Fu, and Zhenbo Luo. R2cnn: rotational region cnn for orientation robust scene text detection. *arXiv preprint arXiv:1706.09579*, 2017. 2
- [17] Chengquan Zhang, Borong Liang, Zuming Huang, Mengyi En, Junyu Han, Errui Ding, and Xinghao Ding. Look more than once: An accurate detector for text of arbitrary shapes. In *Proceedings of the IEEE Conference on Computer Vision and Pattern Recognition*, pages 10552–10561, 2019. 2
- [18] Wei Liu, Dragomir Anguelov, Dumitru Erhan, Christian Szegedy, Scott Reed, Cheng-Yang Fu, and Alexander C Berg. Ssd: Single shot multibox detector. In *European conference on computer vision*, pages 21–37. Springer, 2016. 2
- [19] Joseph Redmon, Santosh Divvala, Ross Girshick, and Ali Farhadi. You only look once: Unified, real-time object detection. In *Proceedings of the IEEE conference on computer vision and pattern recognition*, pages 779–788, 2016. 2
- [20] Minghui Liao, Baoguang Shi, Xiang Bai, Xinggang Wang, and Wenyu Liu. Textboxes: A fast text detector with a single deep neural network. *arXiv preprint arXiv:1611.06779*, 2016. 2
- [21] Minghui Liao, Baoguang Shi, and Xiang Bai. Textboxes++: A single-shot oriented scene text detector. *IEEE transactions on image processing*, 27(8):3676–3690, 2018. 2

- [22] Zhi Tian, Chunhua Shen, Hao Chen, and Tong He. Fcos: Fully convolutional one-stage object detection. In *Proceedings of the IEEE international conference on computer vision*, pages 9627–9636, 2019. 2
- [23] Zengyuan Guo, Zilin Wang, Zhihui Wang, Wanli Ouyang, Haojie Li, and Wen Gao. Location-aware feature selection for scene text detection. *arXiv preprint arXiv:2004.10999*, 2020. 2
- [24] Hei Law and Jia Deng. Cornernet: Detecting objects as paired keypoints. In *Proceedings of the European Conference on Computer Vision (ECCV)*, pages 734–750, 2018. 2
- [25] Chenchen Zhu, Yihui He, and Marios Savvides. Feature selective anchor-free module for single-shot object detection. In *Proceedings of the IEEE Conference on Computer Vision and Pattern Recognition*, pages 840–849, 2019. 2
- [26] Tao Kong, Fuchun Sun, Huaping Liu, Yuning Jiang, Lei Li, and Jianbo Shi. Foveabox: Beyond anchor-based object detection. *IEEE Transactions on Image Processing*, 29:7389–7398, 2020. 2
- [27] Xinyu Zhou, Cong Yao, He Wen, Yuzhi Wang, Shuchang Zhou, Weiran He, and Jiajun Liang. East: an efficient and accurate scene text detector. In *Proceedings of the IEEE conference on Computer Vision and Pattern Recognition*, pages 5551–5560, 2017. 2, 7
- [28] Siyang Qin and Roberto Manduchi. Cascaded segmentation-detection networks for word-level text spotting. In *2017 14th IAPR International Conference on Document Analysis and Recognition (ICDAR)*, volume 1, pages 1275–1282. IEEE, 2017. 2
- [29] Zheng Zhang, Chengquan Zhang, Wei Shen, Cong Yao, Wenyu Liu, and Xiang Bai. Multi-oriented text detection with fully convolutional networks. In *Proceedings of the IEEE Conference on Computer Vision and Pattern Recognition*, pages 4159–4167, 2016. 2
- [30] Cong Yao, Xiang Bai, Nong Sang, Xinyu Zhou, Shuchang Zhou, and Zhimin Cao. Scene text detection via holistic, multi-channel prediction. *arXiv preprint arXiv:1606.09002*, 2016. 2
- [31] Zhuotao Tian, Michelle Shu, Pengyuan Lyu, Ruiyu Li, Chao Zhou, Xiaoyong Shen, and Jiaya Jia. Learning shape-aware embedding for scene text detection. In *Proceedings of the IEEE Conference on Computer Vision and Pattern Recognition*, pages 4234–4243, 2019. 2, 7
- [32] Kaiming He, Xiangyu Zhang, Shaoqing Ren, and Jian Sun. Deep residual learning for image recognition. In *Proceedings of the IEEE conference on computer vision and pattern recognition*, pages 770–778, 2016. 3, 5
- [33] Tsung-Yi Lin, Piotr Dollár, Ross Girshick, Kaiming He, Bharath Hariharan, and Serge Belongie. Feature pyramid networks for object detection. In *Proceedings of the IEEE conference on computer vision and pattern recognition*, pages 2117–2125, 2017. 3
- [34] Enze Xie, Peize Sun, Xiaoge Song, Wenhai Wang, Xuebo Liu, Ding Liang, Chunhua Shen, and Ping Luo. Polarmask: Single shot instance segmentation with polar representation. In *Proceedings of the IEEE/CVF Conference on Computer Vision and Pattern Recognition*, pages 12193–12202, 2020. 5
- [35] Jia Deng, Wei Dong, Richard Socher, Li-Jia Li, Kai Li, and Li Fei-Fei. Imagenet: A large-scale hierarchical image database. In *2009 IEEE conference on computer vision and pattern recognition*, pages 248–255. Ieee, 2009. 5
- [36] Léon Bottou. Large-scale machine learning with stochastic gradient descent. In *Proceedings of COMPSTAT’2010*, pages 177–186. Springer, 2010. 5
- [37] Ilya Sutskever, James Martens, George Dahl, and Geoffrey Hinton. On the importance of initialization and momentum in deep learning. In *International conference on machine learning*, pages 1139–1147, 2013. 5
- [38] Kaiming He, Xiangyu Zhang, Shaoqing Ren, and Jian Sun. Delving deep into rectifiers: Surpassing human-level performance on imagenet classification. In *Proceedings of the IEEE international conference on computer vision*, pages 1026–1034, 2015. 5
- [39] Abhinav Shrivastava, Abhinav Gupta, and Ross Girshick. Training region-based object detectors with online hard example mining. In *Proceedings of the IEEE conference on computer vision and pattern recognition*, pages 761–769, 2016. 5
- [40] Dimosthenis Karatzas, Lluís Gómez-Bigorda, Angelos Nicolaou, Suman Ghosh, Andrew Bagdanov, Masakazu Iwamura, Jiri Matas, Lukas Neumann, Vijay Ramaseshan Chandrasekhar, Shijian Lu, et al. Icdar 2015 competition on robust reading. In *2015 13th International Conference on Document Analysis and Recognition (ICDAR)*, pages 1156–1160. IEEE, 2015. 6
- [41] Wenhai Wang, Enze Xie, Xiaoge Song, Yuhang Zang, Wenjia Wang, Tong Lu, Gang Yu, and Chunhua Shen. Efficient and accurate arbitrary-shaped text detection with pixel aggregation network. In *Proceedings of the IEEE International Conference on Computer Vision*, pages 8440–8449, 2019. 6, 7
- [42] Zhi Tian, Weilin Huang, Tong He, Pan He, and Yu Qiao. Detecting text in natural image with connectionist text proposal network. In *European conference on computer vision*, pages 56–72. Springer, 2016. 7
- [43] Han Hu, Chengquan Zhang, Yuxuan Luo, Yuzhuo Wang, Junyu Han, and Errui Ding. Wordsup: Exploiting word annotations for character based text detection. In *Proceedings of the IEEE international conference on computer vision*, pages 4940–4949, 2017. 7
- [44] Minghui Liao, Zhen Zhu, Baoguang Shi, Gui-song Xia, and Xiang Bai. Rotation-sensitive regression for oriented scene text detection. In *Proceedings of the IEEE conference on computer vision and pattern recognition*, pages 5909–5918, 2018. 7
- [45] Zichuan Liu, Guosheng Lin, Sheng Yang, Jiashi Feng, Weisi Lin, and Wang Ling Goh. Learning markov clustering networks for scene text detection. *arXiv preprint arXiv:1805.08365*, 2018. 7

- [46] Shangbang Long, Jiaqiang Ruan, Wenjie Zhang, Xin He, Wenhao Wu, and Cong Yao. Textsnake: A flexible representation for detecting text of arbitrary shapes. In *Proceedings of the European conference on computer vision (ECCV)*, pages 20–36, 2018. 7
- [47] Wenhai Wang, Enze Xie, Xiang Li, Wenbo Hou, Tong Lu, Gang Yu, and Shuai Shao. Shape robust text detection with progressive scale expansion network. In *Proceedings of the IEEE Conference on Computer Vision and Pattern Recognition*, pages 9336–9345, 2019. 7
- [48] Enze Xie, Yuhang Zang, Shuai Shao, Gang Yu, Cong Yao, and Guangyao Li. Scene text detection with supervised pyramid context network. In *Proceedings of the AAAI Conference on Artificial Intelligence*, volume 33, pages 9038–9045, 2019. 7
- [49] Youngmin Baek, Bado Lee, Dongyoon Han, Sangdoo Yun, and Hwalsuk Lee. Character region awareness for text detection. In *Proceedings of the IEEE Conference on Computer Vision and Pattern Recognition*, pages 9365–9374, 2019. 7
- [50] Yuliang Liu, Lianwen Jin, Shuaitao Zhang, Canjie Luo, and Sheng Zhang. Curved scene text detection via transverse and longitudinal sequence connection. *Pattern Recognition*, 90:337–345, 2019. 7
- [51] Minghui Liao, Zhaoyi Wan, Cong Yao, Kai Chen, and Xiang Bai. Real-time scene text detection with differentiable binarization. In *AAAI*, pages 11474–11481, 2020. 7
- [52] Yuxin Wang, Hongtao Xie, Zheng-Jun Zha, Mengting Xing, Zilong Fu, and Yongdong Zhang. Contournet: Taking a further step toward accurate arbitrary-shaped scene text detection. In *Proceedings of the IEEE/CVF Conference on Computer Vision and Pattern Recognition*, pages 11753–11762, 2020. 7, 8
- [53] Liu Yuliang, Jin Lianwen, Zhang Shuaitao, and Zhang Sheng. Detecting curve text in the wild: New dataset and new solution. *arXiv preprint arXiv:1712.02170*, 2017. 6